Lab-on-chip components for molecular detection

Tijjani Adam, Th S. Dhahi, Mohammed Mohammed, U. Hashim, N. Z. Noriman, and Omar S. Dahham

Citation: AIP Conference Proceedings **1885**, 020194 (2017); doi: 10.1063/1.5002388
View online: http://dx.doi.org/10.1063/1.5002388
View Table of Contents: http://aip.scitation.org/toc/apc/1885/1
Published by the American Institute of Physics

Lab-On-Chip Components for Molecular Detection

Tijjani Adam[1,4,a,), Th S. Dhahi[2,4,b)], Mohammed Mohammed[3,c)], U. Hashim[3,4,d)], N.Z Noriman[1,e)], Omar S. Dahham[1,f]

[1]*Faculty of Technology, Universiti Malaysia Perlis (UniMAP), Kampus Uniciti Alam Sg. Chuchuh, 02100 Padang Besar (U), Perlis, Malaysia*
[2]*Physics Department, College of Science Education, Basra University,Basra, Iraq*
[3]*Center of Excellence Geopolymer and Green Technology, School of Materials Engineering, Universiti Malaysia Perlis (UniMAP), 01007, P.O Box 77, D/A PejabatPosBesar, Kangar, Perlis, Malaysia.*
[4]*Institute of Nano Electronic Engineering (INEE), Universiti Malaysia Perlis (UniMAP), 01000 Kangar, Perlis, Malaysia*

Corresponding Author: [a]tijjani@unimap.edu.my
[b]sthikra@yahoo.com
[c]hmn7575@yahoo.com
[d]uda@unimap.edu.my
[e]niknoriman@unimap.edu.my
[f]eng.omar@mail.com

Abstract. We successfully fabricated Lab on chip components and integrated for possible use in biomedical application. The sensor was fabricated by using conventional photolithography method integrated with PDMS micro channels for smooth delivery of sample to the sensing domain .The sensor was silanized and aminated with 3-Aminopropyl triethoxysilane (APTES) to functionalize the surface with biomolecules and create molecular binding chemistry.The resulting Si-O-Si- components were functionalized with oligonucleotides probe of HPV, which interacted with the single stranded HPV DNA target to create a field across on the device. The fabrication, immobilization and hybridization processes were characterized with current voltage (I-V) characterization (KEITHLEY, 6487). The sensor show selectivity for the HPV DNA target in a linear range from concentration 0.1 nM to 1μM. This strategy presented a simple, rapid and sensitive platform for HPV detection and would become a powerful tool for pathogenic microorganisms screening in clinical diagnosis.

INTRODUCTION

The Lab on Chip is device made up of a transducer and a fluidics component to deliver biological element that is can be an enzyme, an antibody or a nucleic acid to sensing domain [1-8]. The bio-element interacts with the analyte being tested and the biological response is converted into an electrical signal by the transducer[1, 2]. It mechanism can be summarized as follows: when a target molecule comes in close contact with the receptor, non negligible partial charges appear in both the receptor and target molecules[3] This modulates the surface charge profile of the functional layer, which affects the distribution of the electrostatic potential throughout the nanowire[4-6]. This in turn affects the conductance of the nanowire, and thus fluctuations in current can be detected when a voltage is applied at the appropriate terminals [37-44]. The amount of current response depends on the concentration of the target molecule in the liquid [9-15]. Hence, the device suitable for early detection of cancer and related because future developments in early gene specific detection that cause cancer and chronic disease technology offers the potential for improved capabilities over traditional medical diagnosis, prognosis, and treatment [16-25]. The detection of DNA related disease states is steadily rising specific and more accurate information that the other

3rd Electronic and Green Materials International Conference 2017 (EGM 2017)
AIP Conf. Proc. 1885, 020194-1–020194-9; doi: 10.1063/1.5002388
Published by AIP Publishing. 978-0-7354-1565-2/$30.00

methods of detections [26-36]. Thus, the study proposed, the Human Papillomavirus (HPV) Lab on chip that has capability of identify a targeted biomolecule related to (HPV) various.

EXPERIMENTAL

Prior to integration, the transducer surface was modified, since, the transducer is silicon, it required to be modified for the target probe attachment, it was modified with following procedure, using 3-Aminopropyl Triethoxysilane (APTES) as a facilitator to immobilize organic biomolecules on the inorganic surface. 5% APTES in DI water. The 1µl of APTES (0.01M) was dropped on an active area of silicon nanowire device kept for drying in dry cabinet for 3 hrs until it clearly dry. The device further, treated for Human Papillomavirus (HPV) DNA probe attachment and APTES has amine terminated functional group at the end, a modified of 5'end probe with carboxyl group (COOH) was needed onto the surface. 1µM of DNA in deonized distilled water was applied in the active area and incubated for another 3 hours in a moist environment at room temperature. Now the device is ready for HPV virus detection. The PCR product of HPV strain 16 was first denatured into single stranded DNA by heating in thermoshaker for 5 min and then quench to stop the reaction in ice for 5 min. 1 microliters of this single stranded DNA was then applied in active area of silicon nanowires and incubated for 1 h. The sensitivity of the Lab on Chip was examine in a series of solutions with different concentrations of the target ssDNA (HPV). The measured currents of the amine-based probe-DNA-modified silicon nanowire device for target ssDNA concentrations of 0.1, 1, 5, 10, 15, 20, and 25 nM. The integration of silicon nanowire biosensors with microfluidics devices is central to the development of bio sensing chip. Potentially, small-scale and low-density microfluidic networks with individually optimize flow channel and chambers analogous to electronic integrated circuits can enable highly efficient sample preprocessing steps with minimal human input. Small volumes of processed samples are combined with different assay reagents and automatically delivered to integrated sensors for detection and diagnosis. The integration of engineered silicon nanowires with microfluidics devices provides a novel sensing platform that could be used for multiplexed responses of molecules is presented here.It is started with first step which is to activate the surfaces of the PDMS and the silicon substrate in oxygen plasma so that they will permanently bond. Each surface is oxidized in the plasma and covalent siloxane (Si – O – Si) bonds form when the two surfaces are brought into contact.

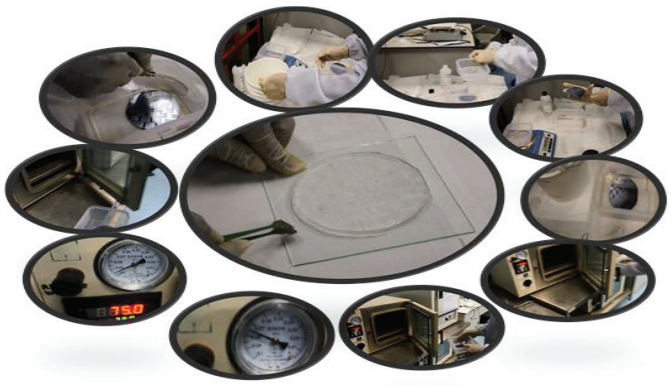

FIGURE 1. Microfluidic surface preparations

The activation is done with a plasma and prior to this, it was clean in cleaner/sterilizer unit, the silicon and PDMS are placed on a glass microscope slide, which is then loaded into the glass chamber of the cleaner. After three minute the, it then loaded plasma spreen and is turned on 250 (watt) power, establishing a pale blue plasma. The inlet valve on the chamber is then slowly opened to let in a small stream of air, turning the plasma pink. We found that a 45 second exposure to the oxygen plasma (after it has turned pink) consistently yielded strong bonds. After 45 seconds, the plasma spreen power is turned off and the chamber is vented, and the pieces are be removed figure 2.

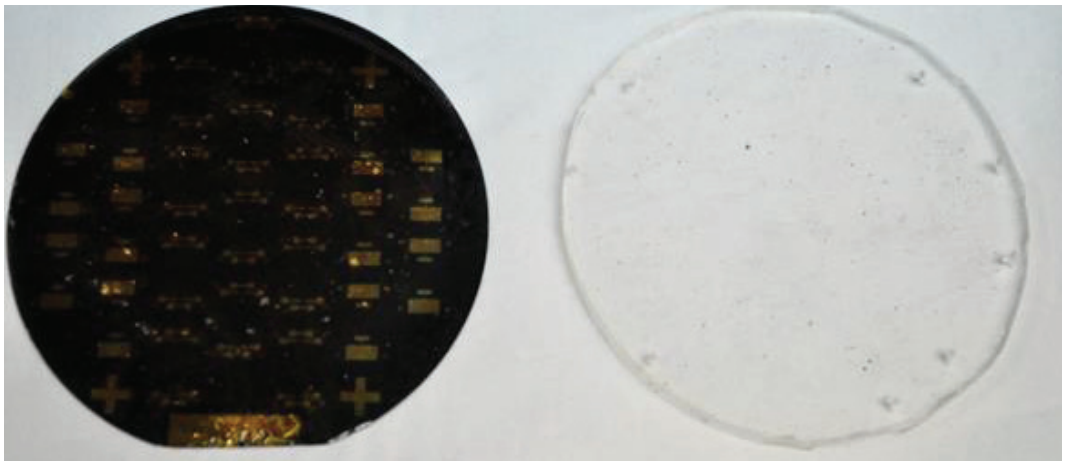

FIGURE 2. Surface activated silicon nanowires and microfluidic devices

Within three minutes of surface activation, the silicon substrate and PDMS pieces must be brought into contact for permanent bonds to form. During this short window of time, they must be precisely aligned before they are brought into contact. To accomplish this, we have developed the following method for alignment using the high resolution mask aligner **FIGURE2**. After the silicon and PDMS surfaces have been plasma activated, these pieces are loaded into the mask aligner using simple adapters. One adapter holds the transparent PDMS in the aligner, where a photo mask would ordinarily go. The other adapter holds the silicon sensor devices below the PDMS in the aligner, where a substrate would ordinarily go. The sensor comes into clear focus as it approaches the height of the PDMS. When the substrate and PDMS are well aligned, they are brought into conformal contact and the surfaces quickly "wet" and form permanent bonds. This method is capable of aligning and bonding the PDMS and substrate with a precision of approximately 1microns.

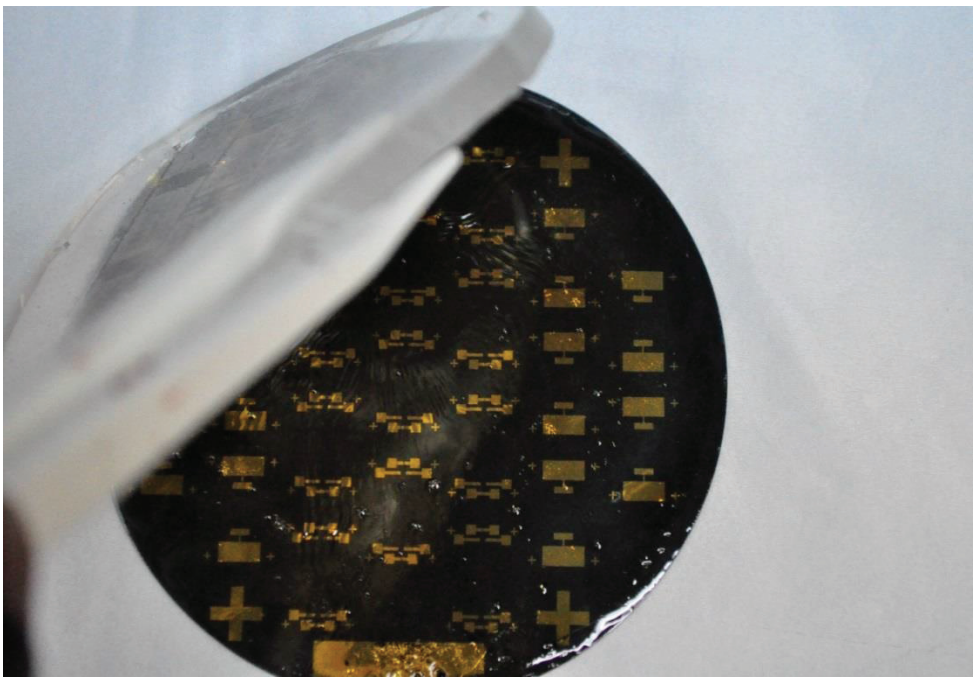

FIGURE 3. Microfluidic alignments on sensor array

The second approach is manual approach with equal precession as mentioned above; the resulting devices were bonded with a PDMS cover in which access holes had already been drilled. Before final bonding, device chips were

cleaned with oxygen plasma at 200W for 1min and immersed in DI water to form hydrophilic surfaces in microfluidic channels which again facilitate the aqueous solution injection during experiment. The device chips were taken out and dried by nitrogen gun figure 3. A piece of fresh PDMS cover with access holes was cleaned in isopropanol (IPA) for 3min assisted by ultrasonic treatment. Finally, the PDMS cover was aligned and pressed onto the device chip to complete bonding process.

BONDING TENSILE TEST

The bonding test was performed by using the tensile strength tester. In order to fit the sample to the gripper of the machine, a piece of PDMS attachment substrate was adhered to both the top and bottom surfaces of the sample. Chloroform was used to attach this attachment substrate to the samples. The evaluation results with various parameters are listed in Table 1. The bonding strength was about 0.015MPa. The results show that the thickness of the interfacial layer does not greatly affect the bonding strength. However, it does affect the bonding quality. Fewer bubbles formed with a thinner PDMS layer. Besides the thickness of PDMS layer, the pre-curing time of PDMS at room temperature also has a significant influence on the bonding quality. Sufficient pre-curing time (~20 hours) is needed to reduce bubble formation and achieves a larger bonded area. A larger bonded area leads to a stronger bonding strength.

TABLE 1. The evaluation results with various parameters

Sample No.	PDMS thickness (μm)	Curing time at room temperature (hr)	Bonding temperature (°C)	Bonding time (hr)	Bonding strength (MPa)	Bonded area (%)	Bubbles formed
1	10	20	90	3	0.015689	100	No
2	25	20	90	3	0.015389	95	Yes
3	35	20	90	3	0.014711	95	Yes
4	10	6	90	1.5	0.011922	90	Yes
5	25	6	90	1.5	0.009900	85	Yes

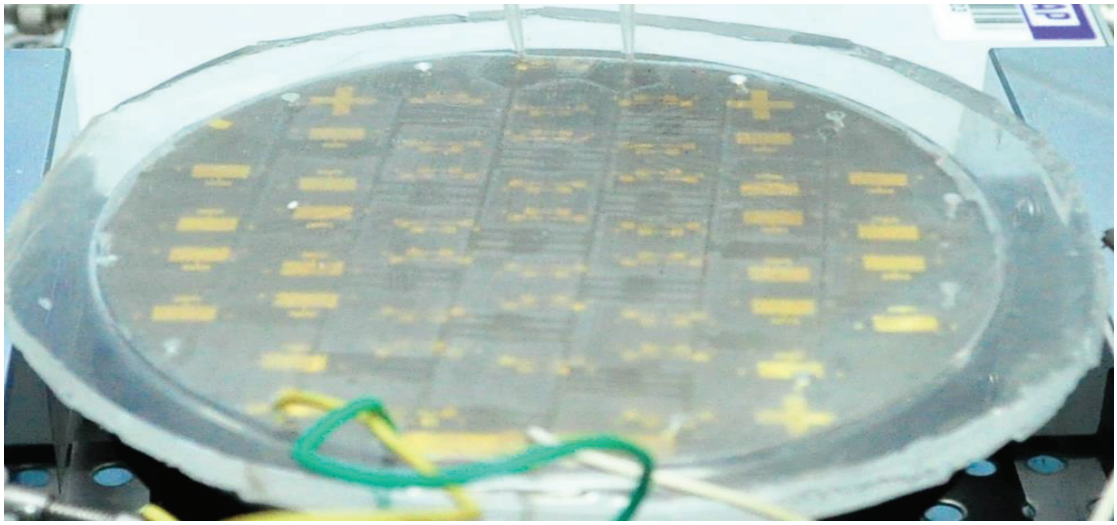

FIGURE 4. Integrated device

BONDING LEAKAGE TEST

The most common concern about microfluidic system is the leakage problem. Many existing polymer-to-polymer substrate bonding methods such as gluing by epoxy or methanol suffered from uneven bonding and leakage near the edge of the device figure 4. Therefore, our fabricated device was tested for leakage. Since both glass and

PDMS are transparent, it is difficult to examine the bonding quality by human eyes. Color dye was pumped into the channel, and no leakage occurred in the channels as shown in figure 5.

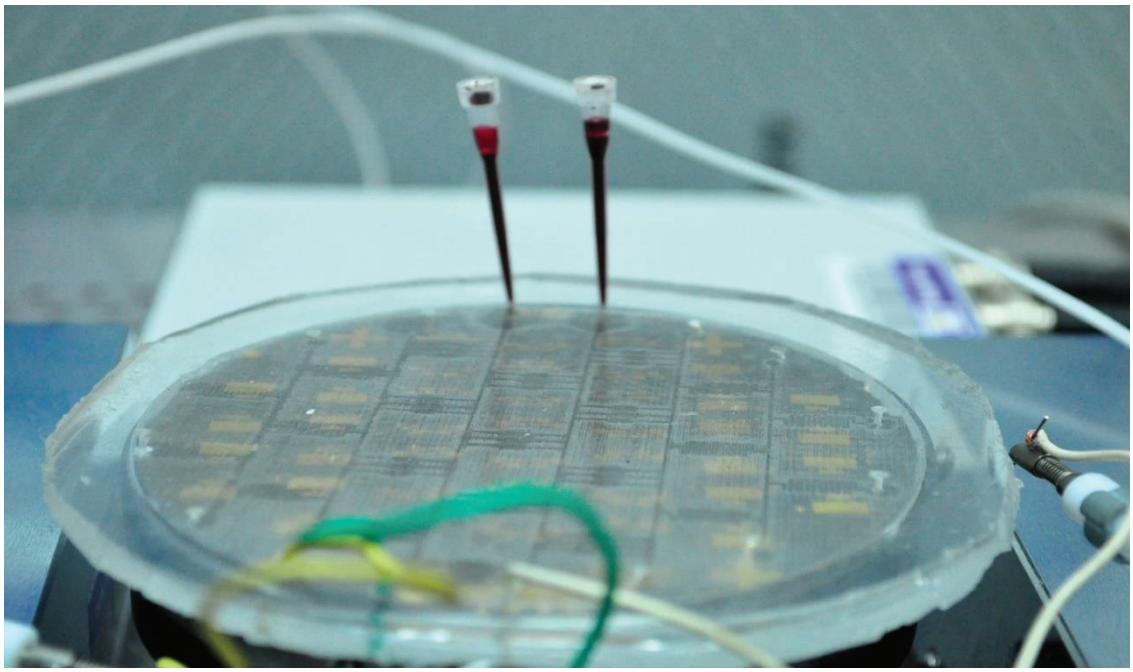

FIGURE 5. Integrated device leakage test

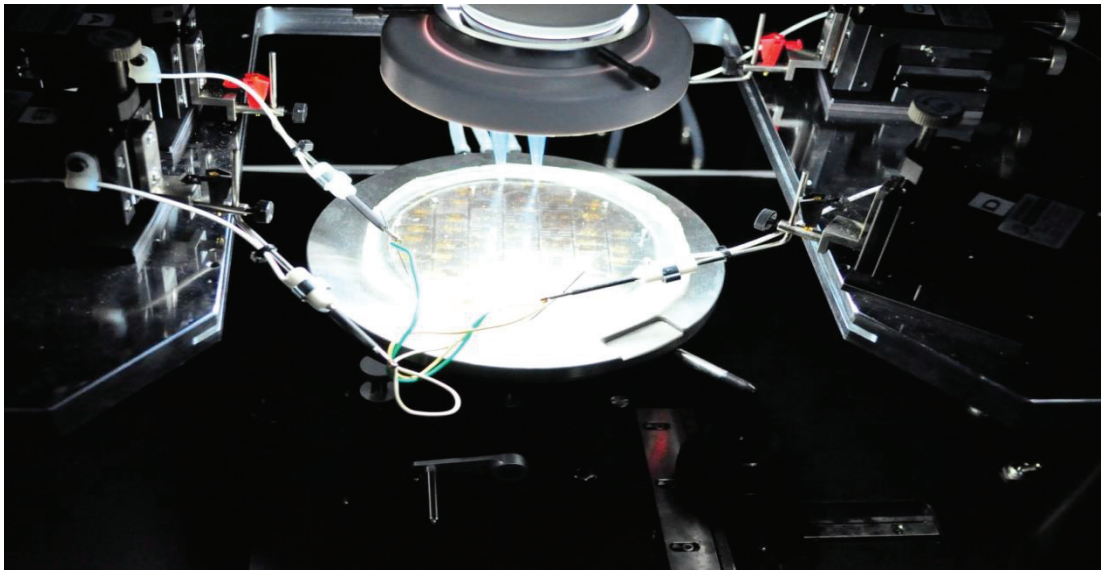

FIGURE 6. Biosensor final electrical tests

RESULTS AND DISCUSSION

From figure 7 we notice the response of the device to SiNW/APTES/ssDNA probe molecule alone give current of $2.15x10^{-10}$. However, when SiNW/APTES/ ssDNA target molecule gives the current $11.73x10^{-9}$A with the same range of voltage, this changes in current value due molecular interaction was reported Adam and Hashim (2014). The reason for this, when a single charged ssDNA target binds to ssDNA probe (receptors) linked via APTES to the

nano transducer, the conductance of a semiconducting nanowire changes from the initial value (Bashouti et al., 2013; Broonstrup et al., 2010) have reported similar argument most of reported literatures based argument due to the localised negative charges of single stranded ssDNA probe. The phosphate ions in ssDNA strands carry a negative charge, which result in electrostatic activities. When the ssDNA unbinds, the conductance returns to the normal value. From the figure 12.The conductance of a second nanowire device without receptors should show lower change during the same time period and it set as reference value. When SiNW was tested the absence of target DNA, there was no detectable signal even after the voltage increased. During I-V characterization for both target and probe, repetitive measurements were conducted for the same sample understand different conditions.

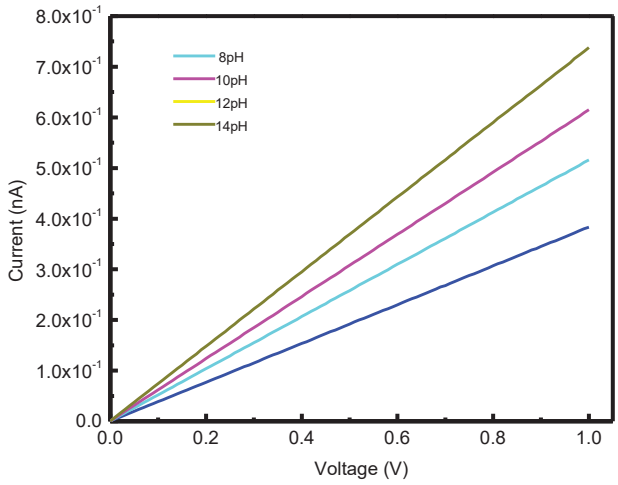

FIGURE 7. Electrical response of silicon-nanowire-based detector to pH from 2 to 14.

The pH-dependent current response was investigated using a standard two-probe I-V measurement set-up. A very low current is expected because of the high resistance of the silicon nanowires. For this purpose, a Keithley 2400 source meter with a current resolution of 10pA was used. To determine the capability of the device, it was treated as a FET and subjected to various pH values. Since the surface of the device is hole-dominated (p-type material), it responds well to pH. In order to further strengthen this response, we protonated the surface of the silicon nanowire in a low-pH fluid to apply a positive surface charge. In particular, in a buffer solution of pH3, on the nanowire surface become positively charged -NH_3^+,which induces mobile carriers (holes) to form inside the nanowire. This approach was proposed by other researchers too. Under these conditions, the nanowire surface acts as a positive top gate affecting the mobile carriers inside the nanowire **FIGURE 7**. For example, when the surface of the silicon nanowire is deprotonated in lower pH liquid, the mobile carriers are depleted accordingly. When the modified p-type Si nanowire device was tested in solutions with pH 2 and 14, it exhibited stepwise increases in conductance. This is consistent with the results of a similar experient performed by many other researchers, where the pH was changed stepwise from 2 to 14 manually using a dropper. In fact, the conductance increased approximately linearly with pH, which is excellent behaviour from the standpoint of sensing. This behaviour results from the presence of two distinct receptor groups that are protonated/deprotonated over different pH ranges: silanol and ammonium groups. From a mechanistic standpoint, the increase in conductance with increasing pH is consistent with a decrease (increase) in the surface positive (negative) charge, which "turns on" the p-type FET through the accumulation of carriers. The key role that the surface receptor plays in defining the response of the nanowire sensors was increasing the surface charge and reducing the resistance of the nanowire. This mechanism was also demonstrated by Lehoucq et al.(2012). In particular, single charged molecules attached to the surface were examined, and the experienced by test charges at the silicon nanowires were simulated at different pH concentrations. The charge accumulation diminishes as the pH decreases and becomes negligible at pH 2 because more silanol surface groups are protonated, resulting in less negative charge on the silicon surface according to the reaction $Si + OH \Leftrightarrow Si - O^- + H^+$. The decrease in surface charge diminishes the charge accumulation as the acid concentration increases (pH decreases), which can be explained by DLVO theory (Adamczyk and Weronski

1999). A high concentration of ions in the medium restricts the ion transfer and leads to more charge accumulation, since electrostatic interactions are stronger thanthe attractive van der Waals forces (Adamczyk and Weronski 1999).

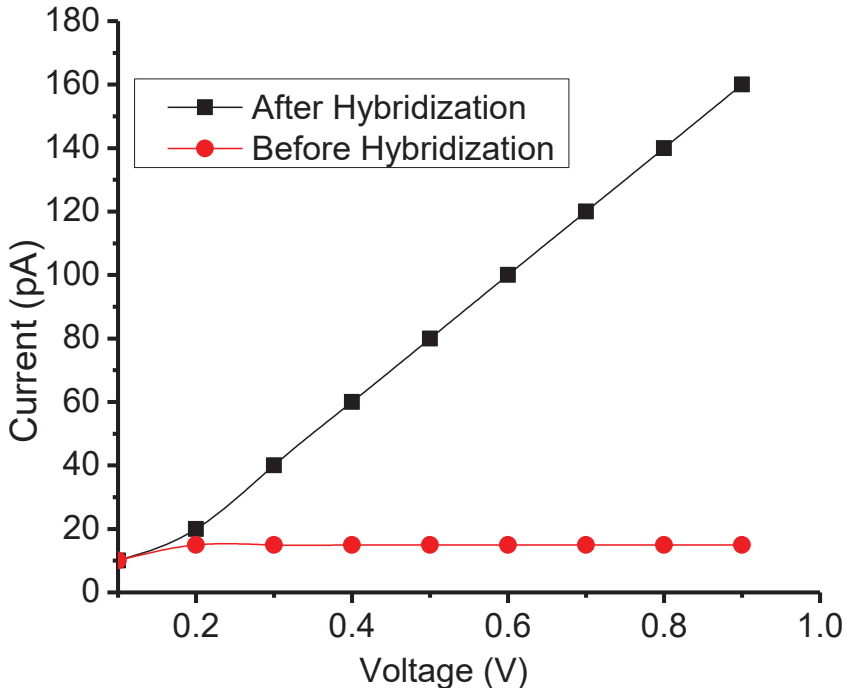

FIGURE 8. Device response for HPV molecules before and after hybridization

Figure 8 show the detection activities data from one device that shows the electronic detection of HPV molecules hybridization. The control chips with exactly the same configuration which was tested prior to hybridization process, in this case when hybridization did not occurred at all its shown no change in conductivity, this can be observed in the same figure. The **I–V** measurements recorded from 0.1 to 1 V across the device, significant increase in current after the capture of HPV molecules.

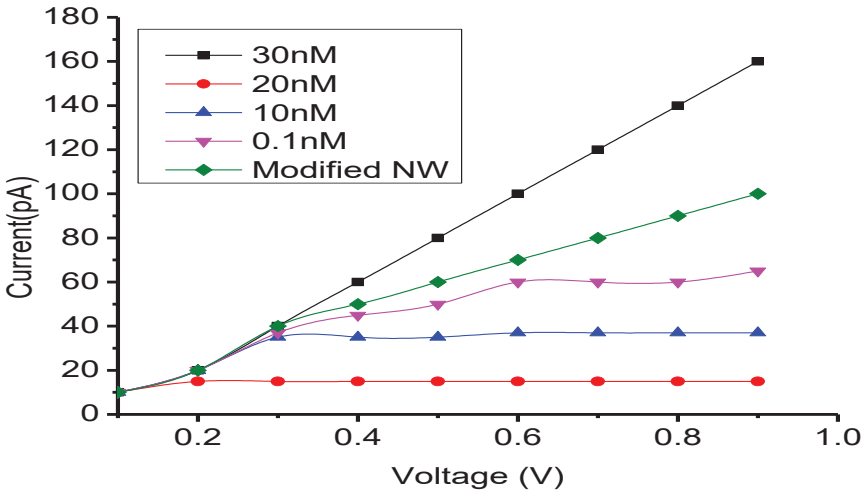

FIGURE 9. Device response to various HPV molecular concentrations

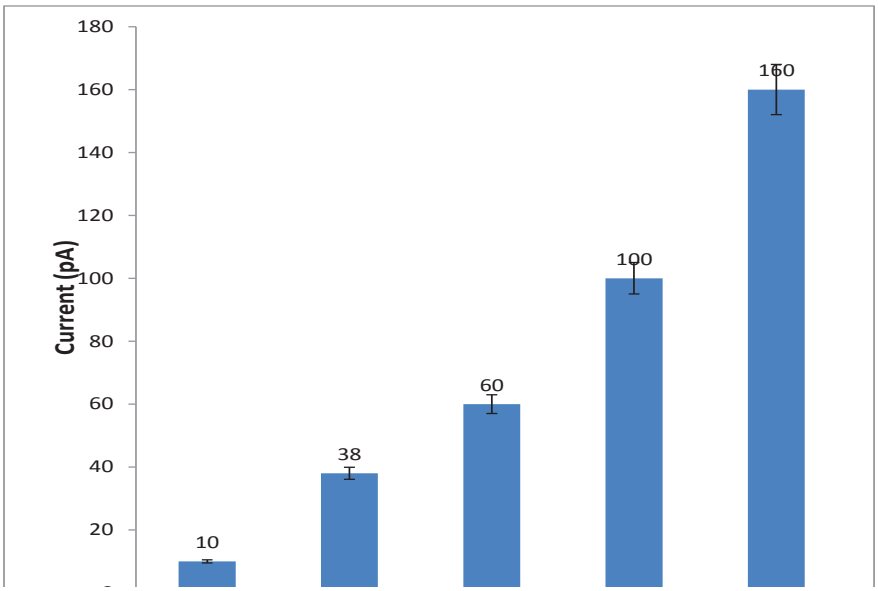

FIGURE 10. Current measured with different concentrations of the targeted DNA. The error calculated standard deviations for repeated current measurements at each concentration.

SUMMARY AND CONCLUSION

Nano Lab on chip framework with precised 20nm sized was developed. The surface was modified for specific molecular detection, the sensor recognizes and captures HPV targeted molecule. The captures HPV targeted molecule is electrically detected. The integration of Nano-wire sensor with micro channels provides rapid, cheap and controlled manufacture of Nano-scale diagnostic tool with high yield. The presence of probe on the sensor surface shows a robust increase in conductivity with increase in HPV molecule concentration. Hence, with its excellent and sensitive detection capability of a DNA linked HPV virus, the device can help in early diagnosis and improved therapy. Such genomic chips can find applications in many electrical sensors for detection of biologically relevant molecules and species.

ACKNOWLEDGEMENT

The authors wish to thank Universiti Malaysia Perlis UniMAP and Ministry of Higher Education Malaysia for giving COE-MTUN grant 901300001 to conduct this research in the Micro & Nano Fabrication Lab. Appreciation also goes to all the team members in the Institute of Nanoelectronic Engineering especially the Nano structure Lab On chip Research Group

REFERENCES

1. A. A. Ensafi, H. Karimi Maleh, S. Mallakpour and B. Rezaei, Colloid Surface B., 87, 480– 488 (2011).
2. A. Sammak, J. Microelectromech S., 16, 912- 918 (2007).
3. A. I. D. Munari, D Vescovi and P. Ciampolini, Solid State Electron., 48, 551-559 (2004).
4. Alan J. H. McGaughey, Eric S. Landry, Daniel P. Sellan, and Cristina H. Amon, Appl. Phys. Lett., 99,131904 (2011).
5. Adam K. Wanekaya, Wilfred Chen, Nosang V. Myung and Ashok Mulchandani, Electroanal., 18, 33 – 550 (2006).
6. T. Adam, U. Hashim, P. L. Leow and Q. H. D, Adv. Mat. Res., 626, 1042-1047 (2013).
7. T. Adam, U. Hashim, P. L. Loew and K. L. Foo, Adv. Sci. Lett., 19, 3454-3458, (2013)
8. Ali A. Ensafi, Hassan Karimi Maleh, S. Mallakpour and M. Hatami, Sensor Actuat. B-Chem., 155, 464–472 (2011).

9. Ali A. Ensafi and H. Karimi Maleh, J. Electroanal. Chem., 640, 75–83(2010).
10. M. Y. Bashouti, K. Sardashti, S. W. Schmitt, M. Pietsch, J. Ristein, H. Haick and S. H. Christiansen, Prog. Surf. Sci., 88, 39–60 (2013).
11. S. M. Berry, L. J. Maccoux and D. J. Beebe, Anal. Chem., 84, 5518–5523 (2012).
12. E. Berthier, E. W. K. Young and D. Beebe, Lab Chip, 12, 1224–1237 (2012).
13. G. Broonstrup, N. Jahr, C. Leiterer, A. Csaki, W. Fritzsche and S. Christiansen, ACS Nano, 4, 7113-7122 (2010).
14. Bruno Sarmento, Francisco M. Goycoolea, Alejandro Sosnik, and Jose dasNeves, International Journal of Carbohydrate Chemistry, 1, 1-12 (2011).
15. C. Herrero Latorre, J. Alvarez Mendez, J. Barciela Garcia, S. Garcia Martin and R. M. Pena Crecente, Anal. Chim. Acta, 749, 16–35 (2012).
16. E. T. Carlen and A. v. d. Berg, Lab Chip, 7, 19-23 (2007).
17. P. S. Chee, R. Arsat, T. Adam, U. Hashim, R. A. Rahim, P. L. Leow, Sensors 12, 12572-12587 (2012) .
18. Y. L. Chueh Cosima, N. Boswell, Chun-Wei Yuan, Swanee J. Shin, Kuniharu Takei, Johnny C. Ho, Hyunhyub Ko, Zhiyong Fan, E. E. Haller, D. C. Chrzan, and Ali Javey, Nano. Lett., 10, 393-397, (2010).
19. Chikara S., Ratan L. and S. K. Joshi, Indian J. Phys. 76A, 325-342, (2002).
20. K. I. Chen, B. R. Li and Y. T. Chen, Nano Today, 6, 131-154 (2011).
21. S. Datta, G. Nandi, A. Bandyopadhyay and P. K. Pal, Int. J. Adv. Manuf. Tech., 45, 276-286 (2009).
22. S. Datta, G. Nandi and A. Bandyopadhyay, J. Manuf. Syst., 28, 55-63 (2009).
23. Darius Andriukaitis and Romualdas Anilionis, "Oxidation Process and Different Crystallographic Plane Orientation Dependence Simulation in Micro and Nano Scale Structures," *Proceedings of the ITI 2007 29th International Conference on Information Technology Interfaces,* (Cavtat, Croatia 2007)
24. D. Li, H. Yamamoto, H. Takeuchi and Y. Kawashima, Eur. J. Pharm. Biopharm., 75, 277–283, (2010).
25. D. Silvestri, N. Barbani, G. D. Guerra, M. Gagliardi and C. Cristallini, Biomed. Eng-App. Bas. C., 22, 509–517 (2010).
26. Das Kanungo, Reinhard Kogler, Peter Werner, Ulrich Gosele, and Wolfgang Skorupa, Nanoscale Res. Lett., 5, 243–246 (2010).
27. E. Taranko, M. Wiertel and R. Taranko, J. Appl. Phys., 111, 023711 (2012).
28. Elahe Afsharmanesh, Hassan Karimi Maleh, Ali Pahlavan and Javad Vahedi, J. Mol. Liq., 181, 8–13 (2013).
29. Eric K. Sackmann, Anna L. Fulton and David J. Beebe, Nature, 507, 181–189 (2014).
30. L. K. Fiddes, N. Raz, S. Srigunapalan, E. Tumarkan, C. A. Simmons, A. R. Wheeler and E. Kumacheva, Biomaterials, 31, 3459-3464 (2010).
31. Foulad gar, Masoud, Karimi Maleh, Hassan, Hosseinzadeh and Rahman, Ionics, 19, 665–672 (2013).
32. Guo Jun Zhang, Li Zhang, Min Joon Huang, Zhan Hong Henry Luo, Guang Kai Ignatius Tay, Eu Jin Andy Lim, Tae Goo Kang and Yu Chen, Sensor Actuat. B-Chem., 146, 138–144 (2010).
33. Guo Jun Zhang and Yong Ning, Anal. Chim. Acta, 49, 1–157 (2012).
34. Hadis Beitollah, Maryam Goodarzian, Mohammad A. Khalilzadeh, Hassan Karimi Maleh, Marjan Hassanzadeh, Mahgol Tajbakhsh, J. Mol. Liq., 173, 137–143 (2012).
35. Hyojin Ko, Jumi Lee,Yongjun Kim, Byeongno Lee, Chan Hee Jung, T. G. Jae Hak Karayiannis, D. Shiferaw, D. B. R. Kenning and V. V. Wadekar, Heat Transfer Eng., (31)4, 257-275, (2010).
36. Jing Tang, Yongcheng Wang, Jun Li, Peimei Da, Jing Geng and Gengfeng Zheng, J. Mater. Chem. A, 2, 6153-6157 (2014).
37. Joseph P. Feser, Jyothi S. Sadhu, Bruno P. Azeredo, Keng H. Hsu and Jun Ma, J. Appl. Phys., 112, 11(2012).
38. Kai Seng Koh, Jitkai Chin , Joanna Chia and Choon Lai Chiang, Micromachines, 3, 427-441 (2012).
39. S. Kar, Appl. Surf. Sci., 252, 3961-3967 (2006).
40. Kuan I Chena, Bor Ran Lia and Yit Tsong Chen, Nano Today, 6, 131–154 (2012).
41. L. De Vico, L. Iversen, M. H. Sorensen, M. Brandbyge, J. Nygard and K.L. Martinez, Nanoscale, 3, 3635–3640 (2011).
42. M. Li, S. Li, J. Wu, W. Wen, W. Li and G. Alici, Microfluid. Nanofluidics, 12 ,751-760 (2012).
43. Linzhi Tang and Nae Yoon Lee, Lab Chip, 10, 1274-1280 (2010).
44. H. Liu and R. M. Crooks, J. Am. Chem. Soc.,133, 17564-17566 (2011).
45. M. P. Marques and P. Fernandes, Molecules, 16, 8368-8401 (2011).